A R C H I V E S O F M E T A L L U R G Y A N D M A T E R I A L S
Volume 53 2008 Issue 3

K. FARYJ*, A. CIAŚ*

MECHANICAL PROPERTIES OF Fe-3Mn-0.8C SINTERED STEELS BASED ON SPONGE AND ATOMISED IRON POWDERS: COMPARISON AND PROBABILISTIC FAILURE PREDICTION

WŁASNOŚCI MECHANICZNE SPIEKANYCH STALI MAGNANOWYCH Fe-3%Mn-0.8%C WYKONANYCH NA BAZIE GĄBCZASTEGO I ROZPYLANEGO PROSZKU ŻELAZA; PORÓWNANIE I PROBALISTYCZNA ANALIZA ZNISZCZENIA

This paper presents a systematic approach to study the effect of manufacturing variables on the mechanical properties of sintered Fe-3Mn-0.8C steel. Tensile and 3 point bending tests have been performed on specimens made of three different iron powders with variations of sintering conditions. Ferro-manganese and graphite powders were admixed to Höganäs sponge, NC100 24, and water atomised, ABC 100.30 and ASC 100.29, iron powders – to produce three variants of Fe-3Mn-0.8C mixtures. The powders were pressed into specimens at 660 MPa, sintered in semi-closed containers for 1 h in dry nitrogen or hydrogen at 1120 or 1250°C, and cooled at 64°C/min. Green and sintered densities were expectedly highest for ABC 100.30 powder at ~7.1 g/cm^3. They were >0.2 g/cm^3 higher than for the sponge powder based specimens. Similarly, Young's modulus in the former material attained ~130 GPa, being ~117 GPa in the latter. Yield strengths were higher for the atomised powder based alloys and for 1250°C and nitrogen sintering. Tensile and bend strengths were somewhat higher for specimens sintered in nitrogen and, generally by ~10%, higher for specimens pressed from sponge iron powder, resulting in ~730 MPa tensile strength for sintering in nitrogen at 1250°C. The strongest ABC 100.30 powder based specimens attained tensile strength ~650 MPa. The higher plasticity of the sponge powder based steel and hence strengths are associated with the increased surface area available to the Mn vapour for alloying. This ensures also cleaner, more cohesive prior powder particle boundaries, the favoured microcracking paths. The study of fracture stress is based on a statistical strength theory suggested by Weibull. It enables fracture probability to be calculated as a function of applied stress. The paper shows that Weibull distribution is more applicable to the strength evaluation and failure statistics of PM steels than the more commonly used normal distribution.
Keywords: sintered steels, strength, quasi-brittle fracture, fracture probability, Weibull analysis

W artykule zaprezentowano systematyczne badania wpływu warunków wytwarzania na własności mechaniczne spiekanych stali Fe-3%Mn-0,8%C. Badania wytrzymałości na rozciąganie i zginanie trójpunktowe przeprowadzono przy użyciu próbek spiekanych w różnych warunkach, wykonanych z trzech różnych proszków żelaza. W celu otrzymania próbek Fe-3%Mn-0,8%C, do redukowanego, gąbczastego proszku żelaza gatunku Höganäs NC 100.24, oraz do rozpylanych proszków żelaza gatunków Höganäs ABC 100.30 i ASC 100.29, wprowadzono mangan w ilości 3%, w postaci proszku żelazomanganu niskowęglowego, oraz grafit w ilości 0,8%. Z proszków sprasowano pod ciśnieniem 660 MPa próbki, które poddano następnie spiekaniu w półhermetycznym pojemniku, w czasie 1 h, w suchym azocie lub wodorze, w temperaturze 1120 lub 1250°C; próbki chłodzono z prędkością 64°C/min. Zgodnie z oczekiwaniami, gęstość tak wyprasek, jak i spiekanych stali była najwyższa w przypadku próbek wytworzonych z proszku ABC 100.30 i wynosiła ~7.1 g/cm^3. Była ona o ponad 0,2 g/cm^3 wyższa, niż gęstość spieków wykonanych z proszku gąbczastego. Podobnie moduł Younga, który osiągał w przypadku pierwszej stali ~130 GPa, podczas gdy w przypadku drugiej ~117GPa. Wartości umownej granicy plastyczności były wyższe w przypadku spieków otrzymanych z rozpylanego proszku żelaza – oraz dla próbek spieczonych w azocie – i próbek spieczonych w temperaturze 1250°C. Wytrzymałość na rozciąganie i zginanie trójpunktowe próbek spieczonych w azocie była wyższa, średnio o ~10%, niż próbek otrzymanych z gąbczastego proszku żelaza, osiągając ~730 MPa w przypadku wytrzymałości na rozciąganie próbek spieczonych w azocie, w temperaturze 1250°C, podczas gdy najmocniejsze próbki wykonane z proszku ABC 100.30 osiągały ~650 MPa. Wyższa plastyczność stali wykonanej z proszku gąbczastego i wyższe jej wytrzymałości związana jest z powiększoną, dostępną dla par manganu, powierzchnią cząstek proszku, co ułatwia wnikanie do nich tego pierwiastka stopowego. Zapewnia to także czyste, bardziej spoiste pierwotne granice cząstek proszku, będące zazwyczaj uprzywilejowanymi ścieżkami mikropęknięć. Badania wytrzymałości oparto na teorii statystycznej zaproponowanej przez Weibulla. Umożliwia ona obliczenie prawdopodobieństwa powstania przełomu w funkcji występującego naprężenia. W artykule wykazano, że do szacowania wytrzymałości stali wytworzonych techniką metalurgii proszków – i do statystycznego opisu tej wytrzymałości – rozkład Weibulla jest bardziej odpowiedni niż, stosowany powszechnie, rozkład normalny.

* FACULTY OF METALS ENGINEERING AND INDUSTRIAL COMPUTER SCIENCE, AGH-UNIVERSITY OF SCIENCE AND TECHNOLOGY, DEPARTMENT OF PHYSICAL AND POWDER METALLURGY, 30-059 KRAKÓW, AL.MICKIEWICZA 30

1. Introduction

Nowadays sintered steel parts are often designed for extremely low failure probability. Mechanical properties of steel structural parts produced by powder metallurgy (PM) depend on many factors. Most of them have a probabilistic character. Weibull statistics procedures can identify which variables need more study. The design process always concerns itself with parts yet to be fabricated and yet to be subjected to loads. These events lie in the future, and the systematic way to appraise the future is via application of probability concepts. Probabilistic approaches are a natural way to solve structural PM parts design problems.

PM manganese steels are relatively new materials, some of which were introduced into service during a period of rapid expansion in the availability of low-cost sintered structural parts. Their reputation suffered badly in the 1990s due to critical sintering condition requirements, poor design and inappropriate powder selection compounded by a lack of processing data [1-3]. Sinter-hardened PM Mn steels are quasi-brittle materials. Their strength should always be considered as a probabilistic quantity [3]. For successful prediction of mechanical failure of structures consisting of sinter-hardened PM steels, a probabilistic approach is indispensable.

Increased iron powder compressibility, resulting in higher green and sintered densities of identically processed powder metallurgy steels of the same chemical composition, generally results in better mechanical properties. This principle should be contrasted with results on manganese steels, for which higher strengths and ductilities have been reported to result from the use of sponge iron powder, to which ferro-manganese and graphite were added [2, 3]. Accordingly it was decided to reinvestigate this "anomalous" behaviour of PM manganese steels.

Recent work at AGH-UST [3-8] has demonstrated that the method of microatmosphere sintering and the design of a semi-closed container are crucial to the attainment of reliable mechanical properties of the PM manganese steel. It was suggested that, compared with Gaussian distribution, the Weibull statistics describes more accurately the distribution of ultimate tensile and transverse rupture strengths of PM steel specimens [9-11]. While the Gaussian distribution is often taken as the accepted statistical distribution for failure strengths there is no theoretical or experimental justification for this situation. When studies of two or more cases are made, the contrast between the probabilities of failure for these cases allows strong analytical focus on the case differences. This strong analytic advantage occurs because all of the assumptions involved in one case can also be carried through for the others in a completely formal way.

2. Experimental procedures

Höganäs sponge NC 100.24, water atomised ABC 100.30, and ASC 100.29 iron powders were the starting materials in this investigation. 0.8% of carbon was introduced as fine Höganäs CU-F graphite and 3% of manganese as Elkem low carbon ferro-manganese. This latter powder is a by-product, <20 μm "fines", from electrode production, of weight % composition 80Mn-1.3C-0.2O-balance Fe. Double-cone mixing and die compaction at 660 MPa, using only die lubrication, of 120 ISO 2740 dog bone specimens, were followed by sintering in dry hydrogen or nitrogen in a horizontal laboratory furnace. Its heat resisting Kanthal APM tube included a water-jacketed rapid convective cooling zone. The dew point of the sintering atmospheres was -60°C (15 ppm moisture). To produce a Mn-rich microclimate (self-gettering effect), the specimens were sintered in a semi-closed stainless steel container with labyrinth seal [4]. Compacts were heated to the sintering temperature, at a rate of 75°C/min., and held at 1120 or 1250°C for 60 min. The convective cooling rate, determined in the temperature range of 1100-500°C, was approximately 64°C/min. After sintering all the specimens were tempered at 200°C for 1 h.

Chemical analyses for oxygen in the iron starting powders and in the sintered alloys were carried out on a Leco apparatus, TC-336 and CS-125, giving ~ 0.2% O and ~0.01 %C for all iron powders.

Standard EN ISO 2740 specimens were tensile tested (R_m) on an MTS 810 servo-hydraulic machine at extension rates of ~ 5 mm/min. The yield strength (also referred to as the proof stress) was measured by the 0.2% offset strain ($R_{p0.2}$). The same specimen types were tested in three-point bending to determine the apparent (uncorrected) transverse rupture strength, TRS. Strength testing was done with span length 28.6 mm, height h = 6 mm, and width b = 6 mm. The crosshead speed of the testing machine was chosen corresponding to a strain rate of 5×10^{-4} s $^{-1}$.

3. Results

3.1. Density and carbon content

In contrast to straight iron-carbon steels, exhibiting swelling, within the (small) experimental error, the densities of Fe-Mn-C compacts remained unchanged on sintering. For ABC 100.30 based steel it was ~ 7.1 g/cm^3,

>0.2 g/cm^3 larger than for the sponge-based alloy (Table 1). As carbon content and density effect strength of PM steel, these parameters were measured (Table 1). Carbon content in the starting powder mixes was 0.8% and after sintering it varied from 0.52 to 0.72%. Carbon losses were directly related to the sintering atmosphere and the sintering temperature.

TABLE 1

Densities and carbon contents after sintering of Fe-3Mn-0.8C steel

Sintering	Carbon content, % and sintered density, g/cm^3					
	NC 100.24		ABC 100.30		ASC 100.29	
	C, %	Density	C, %	Density	C, %	Density
1120°C, H_2	0.62	6.89 ±0.03	0.59	7.11 ±0.02	0.63	6.93 ±0.02
1120°C, N_2	0.72	6.91 ±0.02	0.71	7.09 ±0.06	0.70	6.94 ±0.01
1250°, H_2	0.52	6.91 ±0.03	0.54	7.09 ±0.04	0.54	6.93 ±0.03
1250°C, N_2	0.57	6.91 ±0.01	0.59	7.09 ±0.04	0.58	6.92 ±0.02

± – standard deviation measured on 15 samples

3.2. Mechanical properties

The values of Young's modulus (E), $R_{p0.2}$, R_m, failure strain, and apparent (uncorrected) transverse rupture strengths were determined for at least 15 specimens of each batch. Using the assumption of a normal distribution allows a mean and standard deviation of a random variable to be determined (Tables 2 and 3). The standard deviation is a "natural" measure of statistical dispersion if the centre of the data is measured about the mean.

TABLE 2

Young's modulus and tensile strains (elastic + plastic) to failure of Fe-3Mn-0.8C steel

Sintering	Stress in GPa					
	NC 100.24		ABC 100.30		ASC 100.29	
	E[GPa]	Strain [%]	E [GPa]	Strain [%]	E [GPa]	Strain [%]
1120°C, H^2	116±1	3.7±0.4	130±1	2.7±0.5	119±1	2.5±0.4
1120°C, N_2	117±1	4.2±0.9	129±3	2.6±0.6	119±1	2.7pm0.4
1250°C, H_2	118±2	4.3±0.7	130|pm1	3.2±0.8	119±1	2.8±2.8
1250°C, N_2	117±1	4.6±1.2	129±1	3.1±0.7	118±1	2.9±0.7

± – standard deviation measured on 15 samples

4. Discussion

4.1. Two- and three-parameter Weibull Analysis

Two-parameter and three-parameter Weibull distributions are used to represent the strength distribution of structural PM parts and engineering-designed subassemblies. As PM parts manufacturing processes in the automotive and machinery industry are revised from deterministic to reliability-based design procedures, assessing the goodness-of-fit of these Weibull distributional forms becomes increasingly important.

The three-parameter Weibull distribution has received considerably less attention, probably because the critical two values depend upon the unknown shape parameter. Shapiro-Wilk [12] produced tables of critical values for a test for a Weibull distribution with unknown

TABLE 3

$R_{p0.2}$, R_m and TRS of Fe-3Mn-0.8C steel

Sintering	Stress in MPa								
	NC 100.24			ABC 100.30			ASC 100.29		
	$R_{p0.2}$	R_m	TRS	$R_{p0.2}$	R_m	TRS	$R_{p0.2}$	R_m	TRS
1120°C, H_2	366±53	542±62	1120±138	427±63	524±74	1073±111	413±53	466±52	959±141
1120°C, N_2	441±28	677±50	1357±113	493±57	603±74	1128±89	493±67	565±38	1057±152
1250°C, H_2	440±37	713±68	1337±150	522±79	650±76	1250±196	497±60	578±64	996±93
1250°C, N_2	467±59	732±53	1354±121	518±66	651±67	1244±184	485±88	617±55	1109±134

± – standard deviation measured on 15-26 samples samples

location and scale parameters and a known shape parameter.

4.2. Statistical data reduction and estimation of the Weibull parameters

This discussion is based on a statistical strength theory suggested by Weibull. The Weibull distribution may be more applicable to the evaluation of PM steels than the more commonly used normal distribution since it takes due account of the high and low stress 'tails' of the distribution.

Based on weakest link principle and an empirical function, the cumulative probability of failure of a brittle or semi-brittle material subjected to a stress σ can be represented as the Weibull distribution:

$$P_f = 1 - S = 1 - \exp\left[-\left(\frac{\sigma - \sigma_u}{\sigma_0}\right)^m\right] \text{ for } \sigma \geqslant \sigma_u \quad (1)$$

and $P_f = 0$ for $\sigma < \sigma_u$,

where: P_f is the failure probability, S is survival probability, σ is the failure stress, σ_o is a normalised material strength, σ_u is the threshold stress, and m is the Weibull modulus. This is the basic equation for the failure probability of an uni-axially and uniformly stressed tensile specimen. The 3-parameter Weibull distribution converts known experimental failure data σ_i (i = 1, 2, .. N), by taking $(\sigma_i - \sigma_u)$ of each point and plotting the transformed data. This form of distribution products three parameters: m, σ_u and σ_o. σ_u is the threshold stress bellow which the failure probability is zero and:

$$\sigma_0 = \frac{E - \sigma_u}{\Gamma(1 - 1/m)} \quad (2)$$

where Γ is the Gamma function. The Gamma function is a component in various probability-distribution functions. E is expected value of the distribution function.

The 3-partameter Weibull distribution not only models the actual distribution of strength, but it also predicts a threshold, bellow which none of specimens would be expected to fail. The threshold value could be used to provide a minimum property for the design of PM parts where reliable performance is required. It facilitates also the transfer of strength data of laboratory specimens to situations where the stress distribution is much more complicated.

The threshold value was calculated using maximum likelihood estimation (MLE). For known experimental failure data σ_i (i = 1, 2, . . . N), the parameters σ_u, σ_o and m were determined by maximisation of the likelihood probability density function:

$$L = \prod_{i=1}^{N} f(\sigma_i; \sigma_u; \sigma_0; \mathrm{m}) \quad (3)$$

For calculation the σ_u, σ_o and m from the 3-parameter Weibull distribution following equations were used:

$$N\sigma_0^m = \sum_{i=1}^{N} (\sigma_i - \sigma_u)^m \quad (4)$$

$$\frac{N}{m} - \sum_{i=1}^{N}\left[\left(\frac{\sigma_i - \sigma_u}{\sigma_0}\right)^m \ln\left(\frac{\sigma_i - \sigma_u}{\sigma_0}\right)\right] = \sum_{i=1}^{N} \ln\left(\frac{\sigma_i - \sigma_u}{\sigma_0}\right) \quad (5)$$

$$\left(1 - \frac{1}{m}\right)\sigma_0^m \sum_{i=1}^{N} \frac{1}{\sigma_i - \sigma_u} = \sum_{i=1}^{N} (\sigma_i - \sigma_u)^{m-1} \quad (6)$$

Weibull parameters σ_u, σ_o and m, and correlation factor R^2 (R – Pearson's correlation coefficient) are given in Tables 4 and 5. The 3-parameter Weibull graphs are shown in Fig.1.

Estimation of the Weibull parameters was performed under the constraints $m > 1$ and $0 < \sigma_u < \min\{\sigma_i \ldots. \sigma_N\}$. The second condition stems from the observation that, within the setting of the theory, a failure stress smaller than σ_u is impossible.

The maximum likelihood principle for parameter estimation is intuitively appealing, but for small sample sizes the estimates may be biased. No information is available about the bias of the MLE estimates of the parameters of the Weibull distribution, described strength of PM steels. However, assuming that known results about the bias of the three-parameter Weibull distribution also apply (at least qualitatively) to the present study, the reference value is expected to be biased only slightly, and the Weibull modulus m is underestimated. Whatever the bias of the estimates may be, the plot of the estimated failure probability of the ultimate tensile strength (UTS) and TRS specimens fits the experimental data quite well (Fig. 1).

The smallest fracture stresses recorded during the experiments with the H_2/1120°C NC 100.24 and ASC 100.29 UTS specimens were 410 and 340 MPa, respectively. Compared with this value, the estimate of zero MPa for the threshold stress can be considered as small. However, often, the threshold stress σ_u is assumed in advance to be zero. The advantage of this assumption is that parameter estimation is considerably simplified. However, setting the threshold value to zero is tantamount to restricting the set of admissible parameters, and from mathematics it is known that the maximum of any function over a restricted set is smaller than or, at best, equal to the maximum over the non-restricted set. Consequently, to ensure that the maximum likelihood estimates are actually found, the threshold stress should not be set to zero in advance.

For the sake of completeness, reference will be made also to the less complex 2-parameter analysis. The 2-parameter Weibull distribution (a special case of the 3-parameter distribution for $\sigma_u = 0$) for the failure probability of uniaxially and uniformly stressed tensile specimen is calculated according to

$$P_f = 1-\exp\left[-\left(\frac{\sigma}{\sigma_0}\right)^m\right] \text{ for } \sigma > 0 \text{ and } P_f = 0 \text{ for } \sigma \leqslant 0. \qquad (7)$$

The Weibull modulus is a parameter used to describe the distribution of strength in materials, which break at defects according to weakest link statistics.

There are number of methods for determination of Weibull parameters σ_0 and m from strength measurements, but only two are in common using. In order to find the unknown parameters in a distribution function, the usual way (the most popular method) is the linear regression (least-squares) procedure. For a constant tested volume (specimen gauge length) it is often calculated using a least-squares fit with a weight function on the linearized Weibull equation ln (ln(1/1-P_f)) = $m$ln σ - $m$ln σ_o = $m$ln σ - where $k = m ln\sigma_o$. The Weibull modulus can be determined by plotting ln(ln(1/1-P_f)) against ln σ. The failure probability P_f is estimated by (i-0.3)/(N + 0.4) where N is the total number of specimens and i is the rank number. The weight function used was $w_i = [(1 - P_i) \ln (1 - P_i)]^2$. Weibull parameters σ_o and m as well as R^2 (R – Pearson's correlation coefficient) for the sponge and atomised powder series of specimens are given in Tables 6 and 7.

However, the best estimate of parameters σ_o and m is by the maximum likelihood method, which shows the smallest coefficient of variation (the ratio of the standard deviation and mean of a random quantity). This method allows finding values of m and σ_o and predicting with the highest probability the measured distribution of strengths. This approach has the advantage that it gives the minimum estimation error when the highest and lowest values of strength completely predominate in the analysis, which can lead to serious errors in m values. Since abnormal low or high values of strength can easily arise in stress concentrations in grips, local friction in bending tests etc., this represent a serious drawback. The likelihood of a given probability density function is defined as $L = \prod_{i=1}^{N} f(\sigma_i;\sigma_0;\mathrm{m})$ and thus its log-likelihood function is $\ln L = \sum_{i=1}^{N} f(\sigma_i;\sigma_0;\mathrm{m})$, where N is the number of strength experiments (specimens). Thus, estimates of these parameters can be found by maximising the log-likelihood function. For the 2-parameter Weibull distribution, the equation for determining m from N measures σ_i is

$$\frac{\sum_{i=1}^{N} \sigma_i^m \ln \sigma_i}{\sum_{i=1}^{N} \sigma_i^m} = \frac{1}{m} + \frac{1}{N}\sum_{i-1}^{N} \ln \sigma_i \qquad (8)$$

where m can be obtained by an iterative procedure, and then is calculated by (9)

$$\sigma_0^m = \frac{1}{N}\sum_{i=1}^{N} \sigma_i^m \qquad (9)$$

Using the assumption of the two-parameter Weibull distribution allows m and σ_o to be determined (Tables 8 and 9).

Estimates of m are experimental and therefore subject to scatter. If it is supposed that there is random experimental scatter, it can be shown that there are 2 chances in 3 that the true value of m lies in a range

$$m \pm \frac{m}{\sqrt{2n}} \text{ where } \frac{m}{\sqrt{2n}} \text{ is the standard error.} \qquad (10)$$

The calculated values of the standard error in the Weibull modulus are shown in Table 7. Formula (7) can be used in two ways: first, for estimation of the Weibull parameters on the basis of laboratory data; and second, once these parameters are known, for prediction of the failure probability of other elements (e.g. structural parts). In the latter case, the analysis is usually preceded by a finite element analysis for determination of the stress distribution in the part.

The graphs (Fig. 2) and correlation factors R^2 were obtained from regression output. The value of Weibull modulus, which can be calculated from a test group of specimens, enables the "dependability" of a material to be evaluated numerically. Discontinuities present in the Weibull graphs are expected to be linked to the different defect populations.

4.3. Rationalizing different values of fracture stresses obtained in tensile and bend tests

Fracture stress, also known as fracture strength, is the minimum tensile stress that will cause fracture [13]. It is well-recognized that the value TRS, can exceed that of UTS, of the same PM material, identically processed, by a factor up to ~2, although both these parameters relate to the tensile stress causing fracture. The analysis first takes account of the pre-failure plastic strain, which enables conversion of the nominal strengths, UTS and TRS (representing the peak engineering stresses) to true fracture stresses on the material at the time of rupture.

For simple, three-point, bending of a specimen of width w and thickness t, with the test span l, the TRS relation is: (11)

$$TRS = \frac{3Fl}{2wt^2} \qquad (11)$$

where F is load at failure.

Derivation of this formula assumes linear elastic deformation and the maximum engineering beam tensile stress, $\sigma(B)_{max}$, is equal to TRS only for brittle specimens, as is the case for ceramics. As there is no simple relation in plastically deformed specimens between TRS evaluated by relation (11) and $\sigma(B)_{max}$, it needs to be evaluated [3, 4]:

$$\sigma(B)_{max} = E\epsilon_Y + \omega E(\epsilon_{max} - \epsilon_Y) = E\epsilon_Y + \omega E\epsilon_P. \qquad (12)$$

If $\epsilon_m$ax is not measured directly, provided ω is measured in a tensile test and E, σ_Y, ϵ_Y and TRS evaluated, ϵ_{max} can be derived, e.g. by method of successive approximations, and hence: (13)

$$2TRS_{(\varepsilon\,max)} = E\left\{2\omega\varepsilon_{max} + (1-\omega)\,\varepsilon_Y\left[3 - \left(\frac{\varepsilon_Y}{\varepsilon_{max}}\right)^2\right]\right\} \qquad (13)$$

Formula (13) allows of corrected TRS $_{(\epsilon max)}$ to be determined as shown in Table 7.

TABLE 4

Results of 3-parameter Weibull analysis of UTS measured on 15 samples

Sintering	Iron powder								
	NC 100.24			ABC 100.30			ASC 100.29		
	m	σ_0	σ_u	m	σ_0	σ_u	m	σ_0	σ_u
		MPa			MPa			MPa	
1120°C, H_2	11.4	568	0	2.6	200	345	11.6	487	0
1120°C, N_2	5.5	134	564	2	156	465	1.6	68	504
1250°C, H_2	2.6	176	557	7.5	486	195	1.9	97	479
1250°C, N_2	2.2	120	626	9.2	521	158	2	93	543

TABLE 5

Results of 3-parameter Weibull analysis of UTS measured on 15–26 samples

Sintering	Iron powder								
	NC 100.24			ABC 100.30			ASC 100.29		
	m	σ_0	σ_u	m	σ_0	σ_u	m	σ_0	σ_u
		MPa			MPa			MPa	
1120°C, H_2	1.7	208	988	6.4	540	585	4.03	245	747
1120°C, N_2	3.92	421	976	3.93	422	975	1.96	316	776
1250°C, H_2	2.35	203	1014	3	579	734	4.4	391	639
1250°C, N_2	2.5	313	1077	2	341	969	4.2	529	628

TABLE 6

Results of 2-parameter Weibull analysis of UTS

Sintering	Iron powder								
	NC 100.24			ABC 100.30			ASC 100.29		
	m	σ_0 MPa	R^2	m	σ_0 MPa	R^2	m	σ_0 MPa	R^2
1120°C, H_2	9.56±1.74	570	0.9824	7.83±1.43	556	0.9035	9.54±1.74	490	0.9586
1120°C, N_2	24.61±4.5	698	0.9842	8.95±1.6	636	0.9154	16±2.92	583	0.885
1250°C, H_2	11.69±2.1	743	0.9545	9.24±1.69	685	0.9304	9.96±1.82	607	0.9407
1250°C, N_2	15.37±2.8	756	0.9391	10.49±1.91	682	0.9562	12.09±2.21	642	0.9428

± – standard deviation measured on 15 samples

TABLE 7

Results of 2-parameter Weibull analysis of corrected $TRS_{\varepsilon max}$

Sintering	Iron powder								
	NC 100.24			ABC 100.30			ASC 100.29		
	m	σ_0 MPa	R^2	m	σ_0 MPa	R^2	m	σ_0 MPa	R^2
1120°C, H_2	8.38±1.33	1069	0.9431	9.58±1.55	1013	0.9805	6.84±1.03	909	0,9162
1120°C, N_2	12.0±2.19	1299	0.921	13.21±1.8	1058	0.956	7.17±1.04	1011	0,8706
1250°C, H_2	9.4±1.72	1292	0.9505	6.61±0.94	1222	0.9681	10.84±1.63	927	0,9783
1250°C, N_2	11.89±1.39	1298	0.9421	6.94±0.91	1212	0.9697	8.24±1.24	1058	0,9441

± – standard deviation measured on 15–26 samples

TABLE 8

Comparative Weibull analysis of UTS data. The values of m and σ_0 were calculated for 2-parameter Weibull distribution using linear regression and a least-squares fit method $m_{(L)}$, $\sigma_{0(L)}$, and maximum likelihood method $m_{(M)}$, $\sigma_{0(M)}$

Sintering	Iron powder											
	NC 100.24				ABC 100.30				ASC 100.29			
	$m_{(L)}$	$\sigma_{0(L)}$, MPa	$m_{(M)}$	$\sigma_{0(M)}$ MPa	$m_{(L)}$	$\sigma_{0(L)}$, MPa	$m_{(M)}$	$\sigma_{0(M)}$ MPa	$m_{(L)}$	$\sigma_{0(L)}$, MPa	$m_{(M)}$	$\sigma_{0(M)}$ MPa
1120°C, H_2	9.56 ± 1.74	570	11.40 ± 2.08	568	7.83 ± 1.43	556	6.98 ± 1.27	556	9.54 ± 1.74	490	11.61 ± 2.12	487
1120°C, N_2	24.61 ± 4.5	698	26.91 ± 4.91	698	8.95 ± 1.6	636	9.12 ± 1.66	636	16 ± 2.92	583	17.17 ± 3.13	583
1250°C, H_2	11.69 ± 2.1	743	12.12 ± 2.21	743	9.24 ± 1.69	685	10.72 ± 1.96	683	9.96 ± 1.96	607	10.22 ± 1.82	607 1.87
1250°C, N_2	15.37 ± 2.8	756	15.85 ± 2.89	756	10.49 ± 1.91	682	21.11 ± 2.21	680	12.09 ± 2.21	642	14.74 ± 2.69	640

TABLE 9

Comparative Weibull analysis of $TRS_{\varepsilon max}$ corrected data. The values of m and σ_0 were calculated for 2-parameter Weibull distribution using linear regression and a least-squares fit method $m_{(L)}$, $\sigma_{0(L)}$, and maximum likelihood method $m_{(M)}$, $\sigma_{0(M)}$

Sintering	Iron powder											
	NC 100.24				ABC 100.30				ASC 100.29			
	$m_{(L)}$	$\sigma_{0(L)}$, MPa	$m_{(M)}$	$\sigma_{0(M)}$ MPa	$m_{(L)}$	$\sigma_{0(L)}$, MPa	$m_{(M)}$	$\sigma_{0(M)}$ MPa	$m_{(L)}$	$\sigma_{0(L)}$, MPa	$m_{(M)}$	$\sigma_{0(M)}$ MPa
1120°C, H_2	8.38 ± 1.33	1069	7.90 ± 1.25	1071	9.58 ± 1.55	1013	11.03 ± 1.79	1010	6.84 ± 1.03	909	6.56 ± 0.99	909
1120°C, N_2	12.0 ± 2.19	1299	12.38 ± 2.26	1297	13.21 ± 1.8	1058	12.83 ± 1.75	1059	7.17 ± 1.04	1011	6.20 ± 0.9	1013
1250°C, H_2	9.4 ± 1.39	1292	8.93 ± 1.32	1294	6.61 ± 0.94	1222	6.74 ± 0.95	1222	10.84 ± 1.63	927	10.68 ± 1.61	927
1250°C, N_2	11.89 ± 2.17	1298	10.64 ± 1.48	1300	6.94 ± 0.91	1212	7.41 ± 0.97	1211	8.24 ± 1.24	1058	8.6 ± 1.3	1056

5. Conclusions

1. Suitability of sintering Fe powder mixed with low-carbon ferromanganese and graphite in dry nitrogen (or hydrogen) atmosphere in semi-closed containers to produce Fe-3Mn-0.8C steel has been confirmed. Industrial development of nitrogen sintering of Mn steels will have positive safety and economic implications.
2. Tensile strains to failure, and values of UTS and TRS were always highest for the sponge-based alloys, similarly processed to those based on atomised irons, reaching 4.6%, 730 and 1350 MPa, respectively.
3. Young's moduli and yield strengths reflected densities of the materials, with the best values, 130 GPa and 522 MPa, respectively, recorded for ABC 100.30 based steel.
4. Expectedly all properties of steels emanating from ABC 100.30 were superior to those from ASC100.29.

5. Mechanical properties of steels sintered at 1250°C, with all other compositional and processing parameters remaining the same, in spite of lower carbon contents, were superior to those sintered at 1120°C.
6. Weibull analysis is a sound method to analyse strengths of structural PM Mn steels. It can be developed into an important tool for helping understand the physical processes involved. One of the great advantages of the Weibull analysis method is that it allows a means of predicting the likelihood of failure of a material at low stress values possibly allowing engineers to select a material depending on the expected level of stress. Finely, three-parameter Weibull analysis can be apply to predict the cumulative failure probability, and the threshold stress, for fracture of the tested specimens.

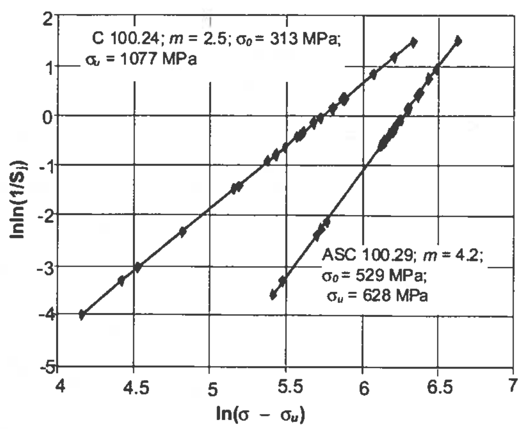

Fig. 1. Comparative plots of fit to three-parameter Weibull distribution for TRS

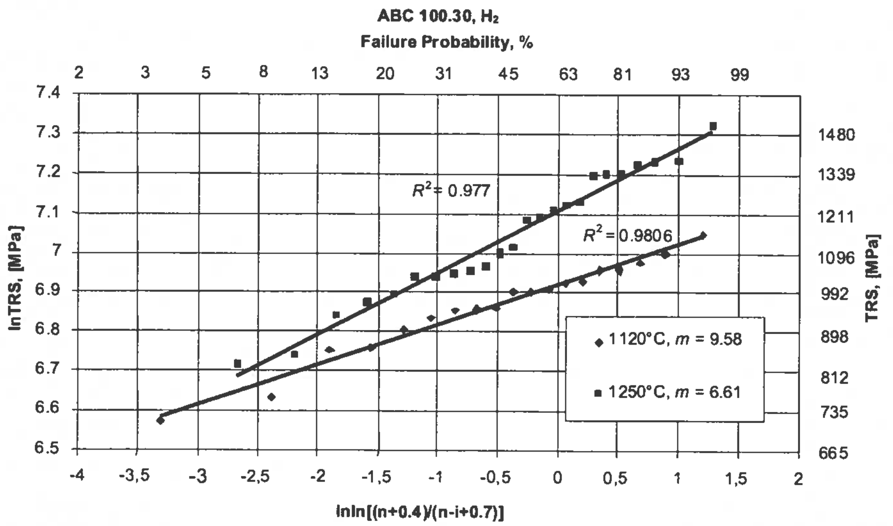

Fig. 2. Two parameter Weibull graphs; m (given by slope), R^2 (correlation factor), and the scale factor σ_o were obtained using regression tool

Acknowledgements

The work described forms part of the programme supported by a KBN contract No. 11.11.110.788.

REFERENCES

[1] A. S a l a k, Ferrous Powder Metallurgy. Ed. Cambridge International Science Pub. (1995).
[2] M. S u ł o w s k i, A. C i a ś, Inżynieria Materiałowa **4**, 1179-1183 (1998).
[3] A. C i a ś, Development and Properties of

Fe-Mn-(Mo)-(Cr)-C steels. Ed. Uczelniane Wydawnictwo AGH, Kraków (2004).
[4] A. Ciaś, S. C. Mitchell, A. Watts, A.S. Wronski, Powder Met. **42**, 227-233 (1999).
[5] A. Ciaś, S. C. Mitchell, K. Pilch, H. Ciaś, M. Sułowski, A. S. Wronski, Powder Metallurgy **46**, 165-170 (2003).
[6] S. C. Mitchell, A. Ciaś, Powder Metallurgy Progress **4**,132-142 (2004).
[7] A. Ciaś, S. C. Mitchell, Powder Metallurgy Progress **5**, no. 2, p. 82-91 (2005).
[8] A. Ciaś, A. S. Wronski, Powder Metallurgy Progress **7**,139-149 (2007).
[9] J. W. Newkirk, S. Thakur, Powder Met. **45**, p. 354-358 (2002).
[10] A. S. Wronski, A. Ciaś, Powder Metallurgy Progress **3**, 119-127 (2003).
[11] A. S. Wronski, A. Ciaś, PM 2004 World Congress & Exhibition, Vienna 17-21 October **3**, 1-6 (2004).
[12] S. S. Shapiro, W. B. Wilk, H. Chen, Journal of the American Statistics Association **63**, 1343-1354 (1968).
[13] McGraw-Hill Dictionary of Scientific and Technical Terms, 6th edition, McGraw-Hill (2003).

Received: 20 June 2008.